Evolution of inbreeding avoidance and inbreeding preference through mate choice among interacting relatives

Supplementary Material for the *American Naturalist*

A. Bradley Duthie[1,*], Jane M. Reid[1]

[1] Institute of Biological and Environmental Sciences, School of Biological Sciences, Zoology Building, Tillydrone Avenue, University of Aberdeen, Aberdeen AB24 2TZ, United Kingdom [*] E-mail: aduthie@abdn.ac.uk, brad.duthie@gmail.com, jane.reid@abdn.ac.uk

Keywords: Inbreeding strategy, mate choice, mating system, reproductive strategy, relatedness, fitness

---

This online appendix presents the following for an individual-based model of biparental inbreeding: 1) extended model results, 2) extended analysis of effective population size N_e, 3) sensitivity analyses on model parameters, 4) evidence for runaway evolution of inbreeding avoidance, and 5) temporal dynamics of simulations. In the model, additive alleles underlying either inbreeding avoidance S^A or inbreeding preference S^P are allowed to mutate within a population initially fixed for inbreeding tolerance S^+. Simulations proceed for 3000 generations, and the end frequency of alleles underlying active inbreeding strategies is recorded. In all simulations, either females or males choose mates. Inbreeding load is simulated explicitly with deleterious recessive alleles L^- mutating from wild type alleles L^+ at 1000 loci. Neutral mutant alleles N^- are modelled at a single locus, and reach an expected frequency of $N^- = 0.5$ after 3000 generations.

Table of contents

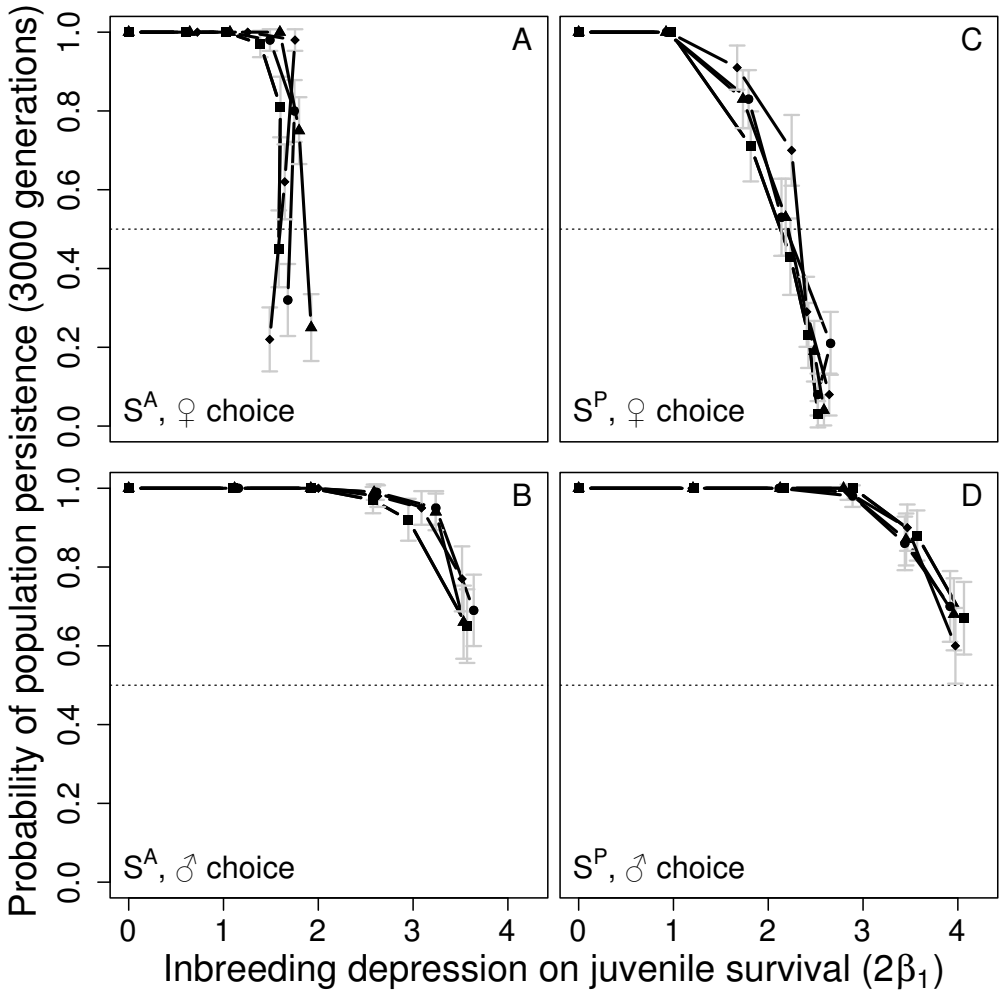

Figure S1: Proportion of simulations where populations persisted for 3000 generations when (A) females and (B) males were the choosing sex given the introduction of a mutant allele underlying inbreeding avoidance S^A, and when (C) females and (D) males are the choosing sex given the introduction of a mutant allele underlying inbreeding preference S^P. Six selection coefficients against deleterious recessives (s) were simulated (connected points), causing inbreeding depression (expressed as diploid lethal equivalents, $2\beta_1$). Error bars show 95% confidence intervals around proportions; 95% CIs around $2\beta_1$ were negligible (< 0.01). Connected points show simulations where the haploid cost of inbreeding avoidance or preference (c) was 0.000 (■), 0.0025 (●), 0.0050 (▲), and 0.0100 (◆). Equivalent s values caused lower $2\beta_1$ given mutant S^A alleles (A,B) rather than given mutant S^P alleles (C,D), as reflected in greater separation between points on the x-axis given mutant S^P alleles. At equivalent s, a higher proportion of populations with S^A persisted compared to S^P, but populations with S^P had a higher probability of persisting at equivalent $2\beta_1$. Probability of population persistence was lower when females chose mates (A,C) because immigrants were of the non-choosing sex, so when males chose (B,D), females were added to the population. Males mate multiply, so these immigrant females produced additional outbred offspring increasing the probability of persistence.

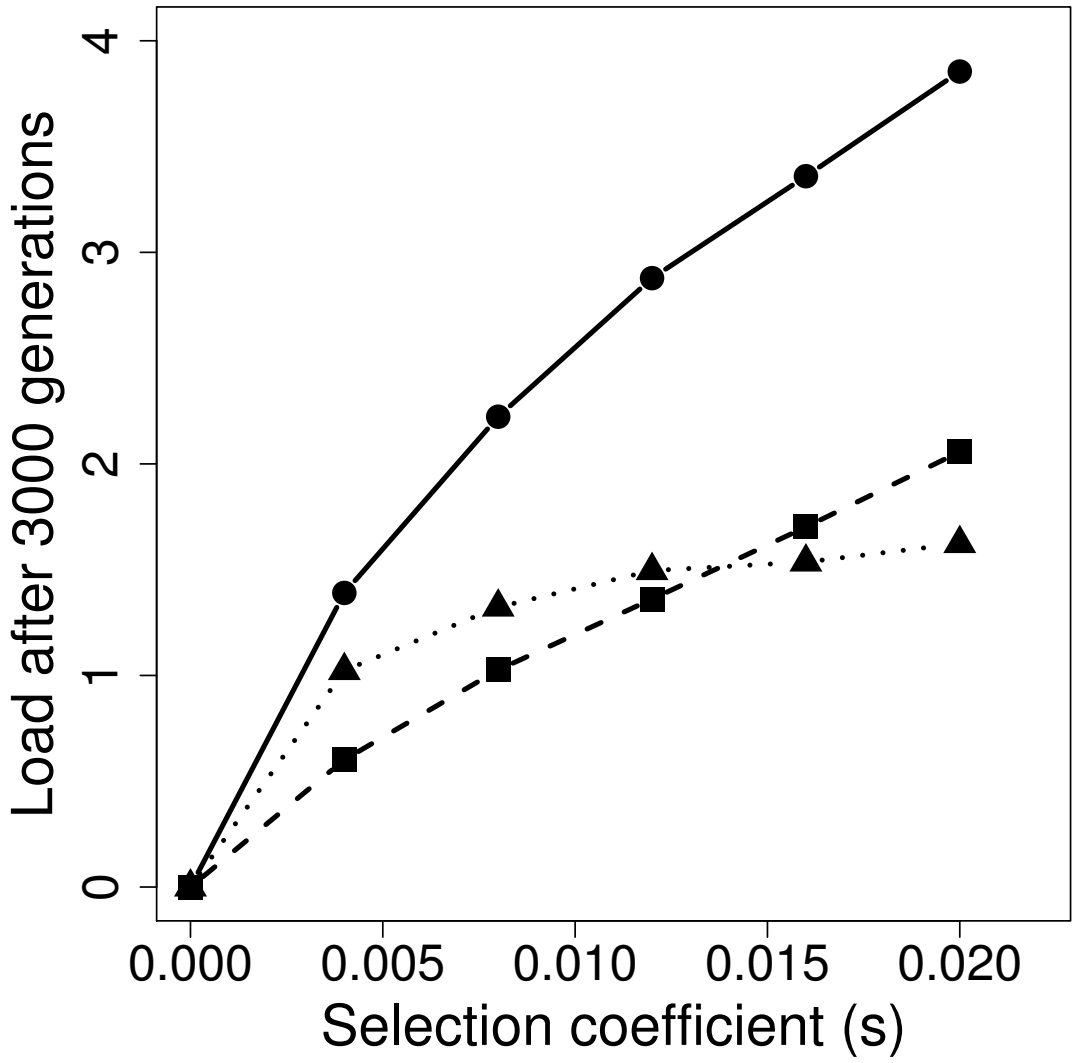

Figure S2: Selection coefficients (s) against deleterious recessive alleles L^- are shown versus different metrics of load, as obtained when a mutant allele S^A underlying inbreeding avoidance is introduced and females choose mates. After 3000 generations, mutation load defined as the mean haploid lethal equivalents per individual was calculated directly from individual genotypes (●; solid). Load attributable to inbreeding (β_1; ■; dashed) versus load independent of inbreeding (β_0; ▲; dotted) was estimated by regressing the natural log of offspring survival probability (Ψ) against offspring inbreeding coefficients (f_{off}) such that $\ln(\Psi) = \beta_0 + \beta_1 f_{\text{off}}$. Each s value includes 67-100 replicate simulations (fewer than 100 where populations went extinct); 95% confidence intervals around load values were negligible and are not show.

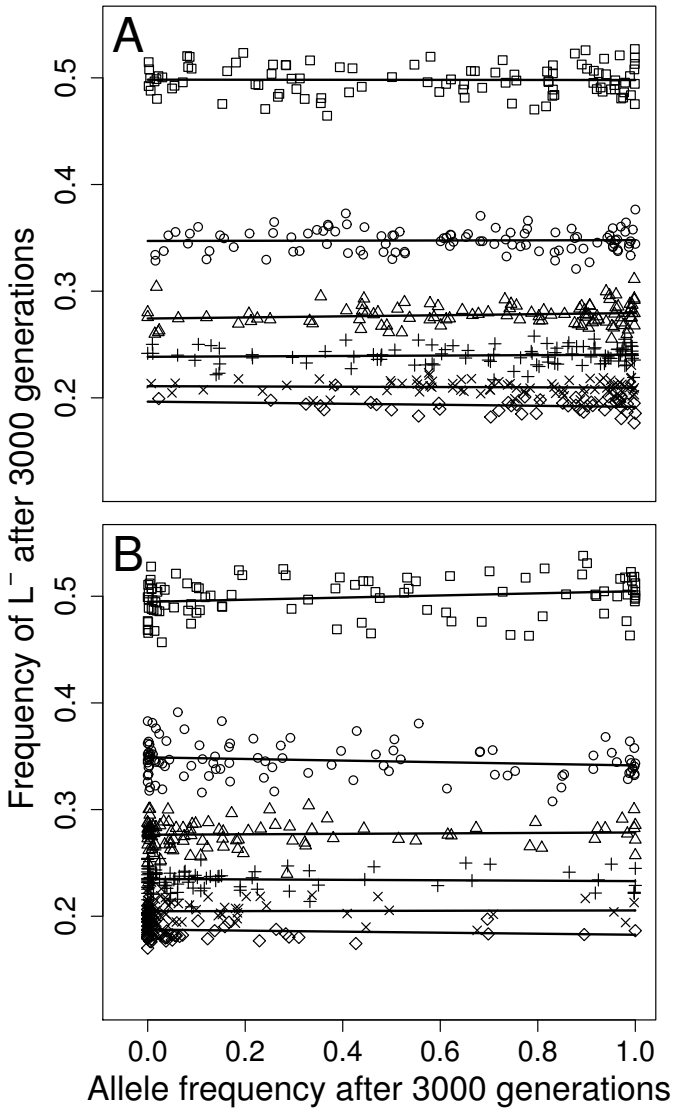

Figure S3: End frequencies of deleterious recessive alleles (L^-) versus the end frequencies of (A) inbreeding strategy alleles underlying inbreeding avoidance S^A and (B) inbreeding preference S^P when females choose mates and after 3000 generations in independent simulations over different selection coefficients against deleterious recessive alleles (s): $s = 0.000$ (□), $s = 0.004$ (○), $s = 0.008$ (△), $s = 0.012$ (+), $s = 0.016$ (×), and $s = 0.020$ (◇). Solid lines show regressions through different s points; regression lines are not shown in (B) where $s = 0.020$ because only 3 points were available. There was no cost associated with alleles underlying active inbreeding strategies (i.e., $c = 0$). Results were not qualitatively different when males chose mates. The end frequency of L^- did not vary markedly with the end frequency of S^A or S^P. There was therefore little evidence of coevolution between inbreeding strategy and inbreeding load, or consequently of purging.

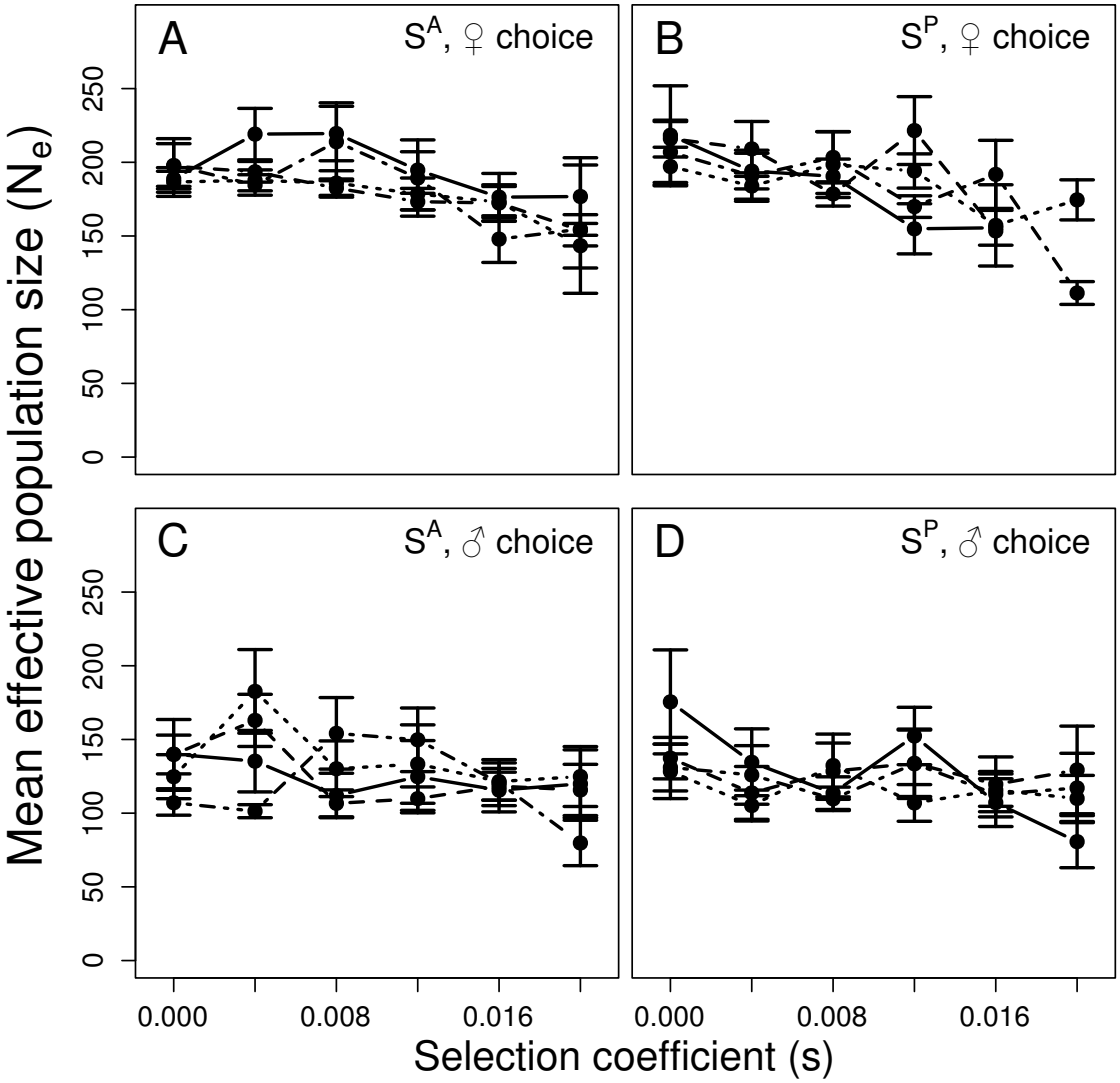

Figure S4: Mean effective population size (N_e) across all parameter combinations when a mutant allele underlying inbreeding avoidance (S^A; A & C) or inbreeding preference (S^P; B & D) is introduced in a population initially fixed for an allele underlying random mating (S^+). Simulations include mate choice enacted by females (A & B) and males (C & D) across different selection coefficients (s). Different lines show different costs of S^A or S^P alleles, including 0 (solid), 0.0025 (dashed), 0.005 (dotted), and 0.010 (dot-dash); error bars show standard errors. These results show simulations from primary results using default parameter values. Because N_e is unaffected by cost, values of c are pooled to show how N_e differs among default parameters for different mutant S^A or S^P and female or male choice across values of s in Figure S5. This faciltiates comparison of N_e for different choosing sex scenarios.

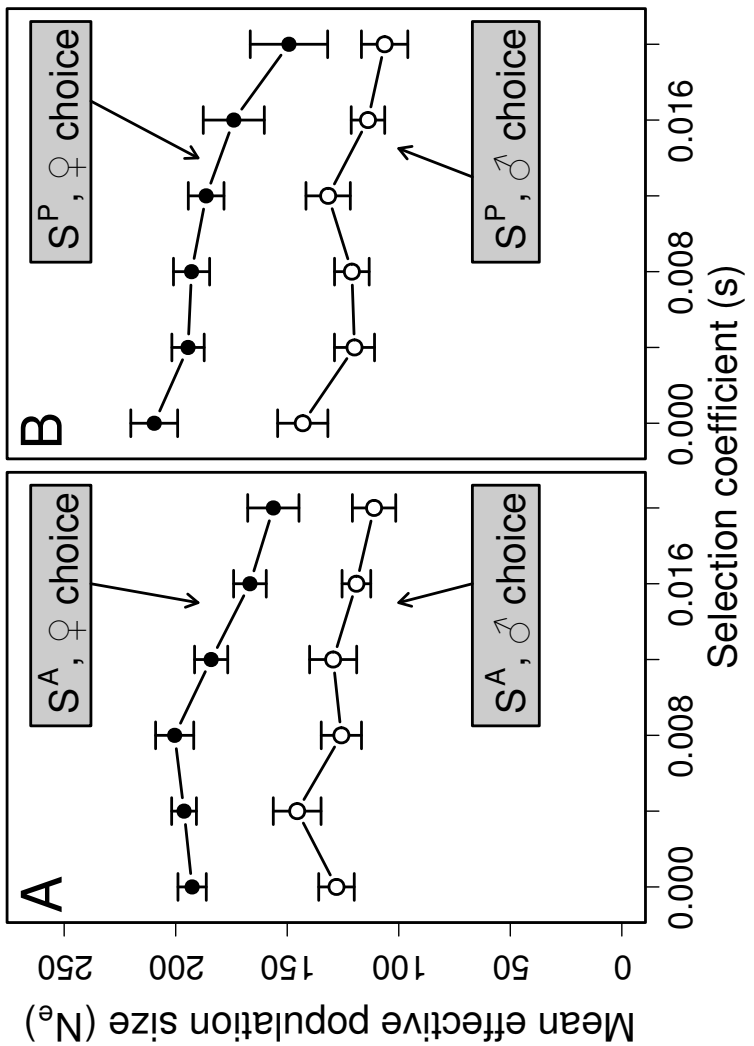

Figure S5: Mean effective population sizes (N_e) when females (black points) and males (white points) choose mates given a mutant allele underlying inbreeding avoidance (S^A; A) and inbreeding preference (S^P; B). Connected points show how N_e varies across different selection coefficients against deleterious recessive alleles (s). Values of S^A or S^P costs ($c = \{0, 0.0025, 0.005, 0.01\}$) had no effect on N_e (see Figure S4), and are pooled for all points to more clearly show the difference between choosing sex scenarios. Each point therefore represents the mean of a unique set of parameter combinations across a pooled c, and error bars show standard errors. Overall, these results show that N_e decreased weakly with increasing s; this was caused by stronger inbreeding depression at high s reducing population size. Most noticeable is that N_e was lower when males chose mates than when females chose mates. This was caused by a higher variation in male reproductive success when males chose.

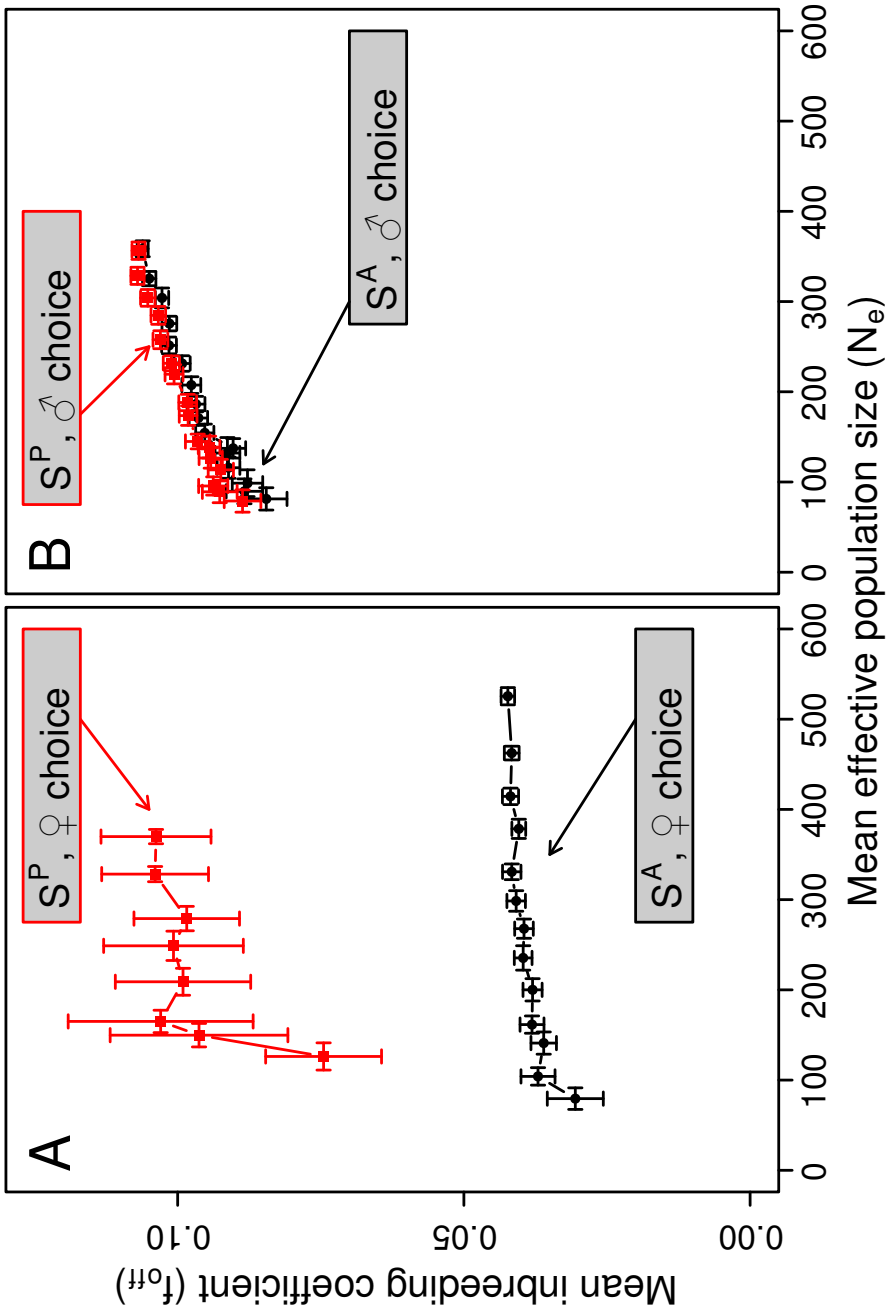

Figure S6: Mean offspring inbreeding coefficient (f_{off}) for simulations with mutant alleles underlying inbreeding avoidance (S^A; black) or preference (S^P; red) given different effective population sizes (N_e). Points shows 100 replicate simulations when either females (A) or males (B) were the choosing sex. Replicate simulations have identical parameter values, including identical selection coefficients against deleterious recessive alleles ($s = 0.012$) and direct costs on inbreeding strategy ($c = 0.0025$). Different effective population sizes are produced by uniformly varying female and male carrying capacities (K_f & K_m). Error bars show 95% confidence intervals. Overall, f_{off} varied vary little with N_e (note the scale of the y-axis). The slight increase with N_e occurred because the number of immigrants per generation (ρ) was constant across all simulated carrying capacities.

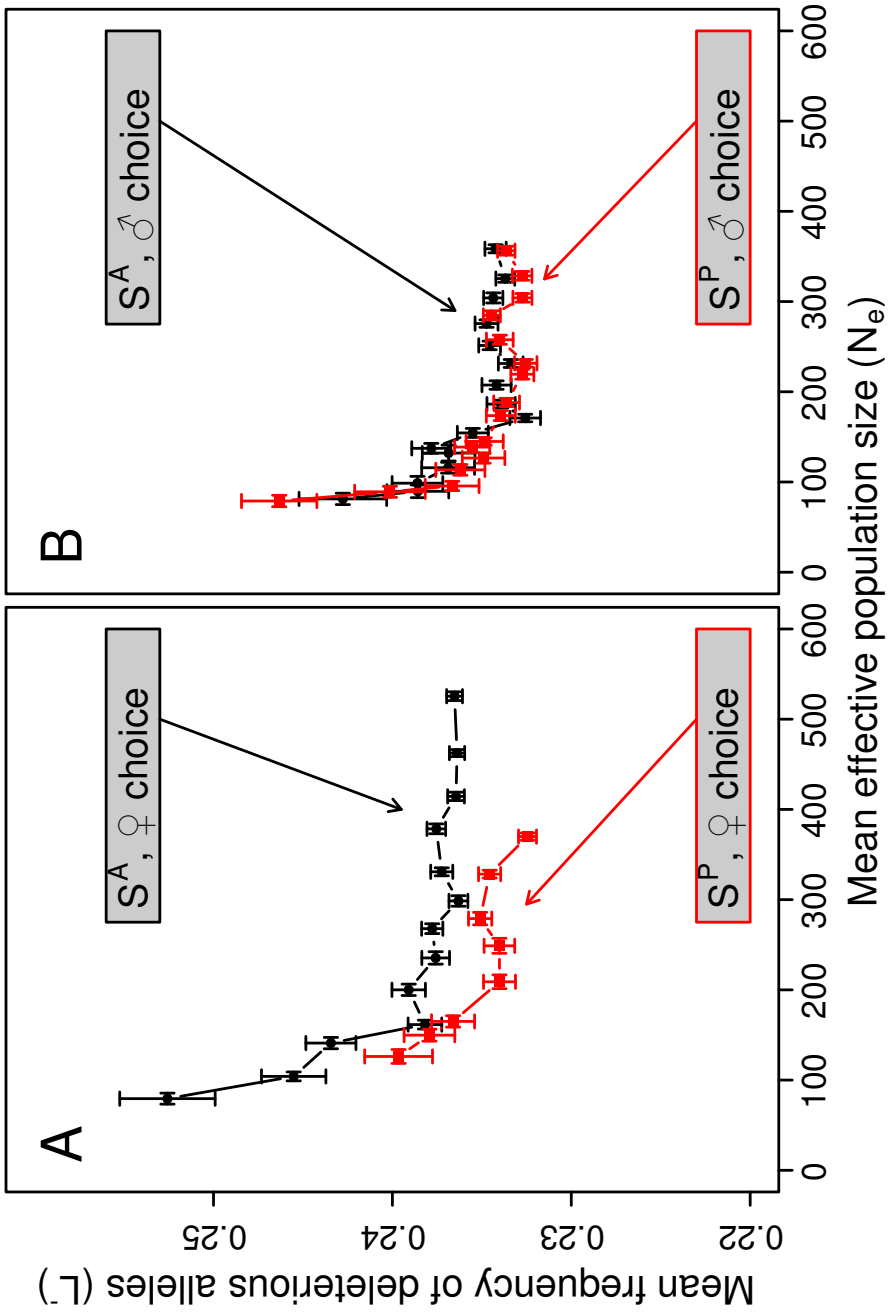

Figure S7: Mean deleterious recessive allele frequency (L^-) for simulations with mutant alleles underlying inbreeding avoidance (S^A; black) or preference (S^P; red) given different effective population sizes (N_e). Replicate simulations have identical parameter values, including identical selection coefficients against deleterious recessive alleles ($s = 0.012$) and direct costs on inbreeding strategy ($c = 0.0025$). Different effective population sizes are produced by uniformly varying female and male carrying capacities (K_f & K_m). Error bars show 95% confidence intervals. Overall, the frequency of L^- varied very little with N_e (note the scale of the y-axis). The slight decrease in L^- frequency with increasing N_e was likely caused by stronger selection relative to drift.

How to interpret Figures S8-S16

Figures S8-S16 show results across a range of parameter combinations in order to address sensitivity of end allele frequencies to parameter values. Below, a description is provided to explain how the data presented in these figures should be interpreted. Individual figure legends then provide specific interpretations of model results.

Figures show distributions of end frequencies of alleles underlying inbreeding avoidance (S^A) and inbreeding preference (S^P) when females and males choose mates in populations after 3000 generations. Large columns present results with a mutant S^A where females choose, a mutant S^A where males choose, a mutant S^P where females choose, and a mutant S^P where males choose mates. Within each large column, the four left-hand columns present results with different direct costs (c) of mate choice. Rows present results with different selection coefficients (s) against deleterious recessive alleles. Each box therefore presents 100 replicate simulations for a unique set of parameter combinations, and points within boxes show mean end allele frequencies for a single simulation. Boxes with fewer than 100 points reflect extinction, and missing boxes reflect extinction of all replicates. Along the y-axis, points show end allele frequencies from 0-1. Points are randomised on the x-axis to facilitate visualisation; the x-axis therefore does not convey information. Solid horizontal red lines show mean end allele frequencies, and red shaded regions show 95% bootstrapped confidence intervals around the means. Solid blue lines show expected end frequencies under mutation-drift balance (0.5). For comparison, blue points on the right-hand boxes of A-D show the distribution of mutant neutral allele (N^-) end frequencies across replicates where $c = 0$.

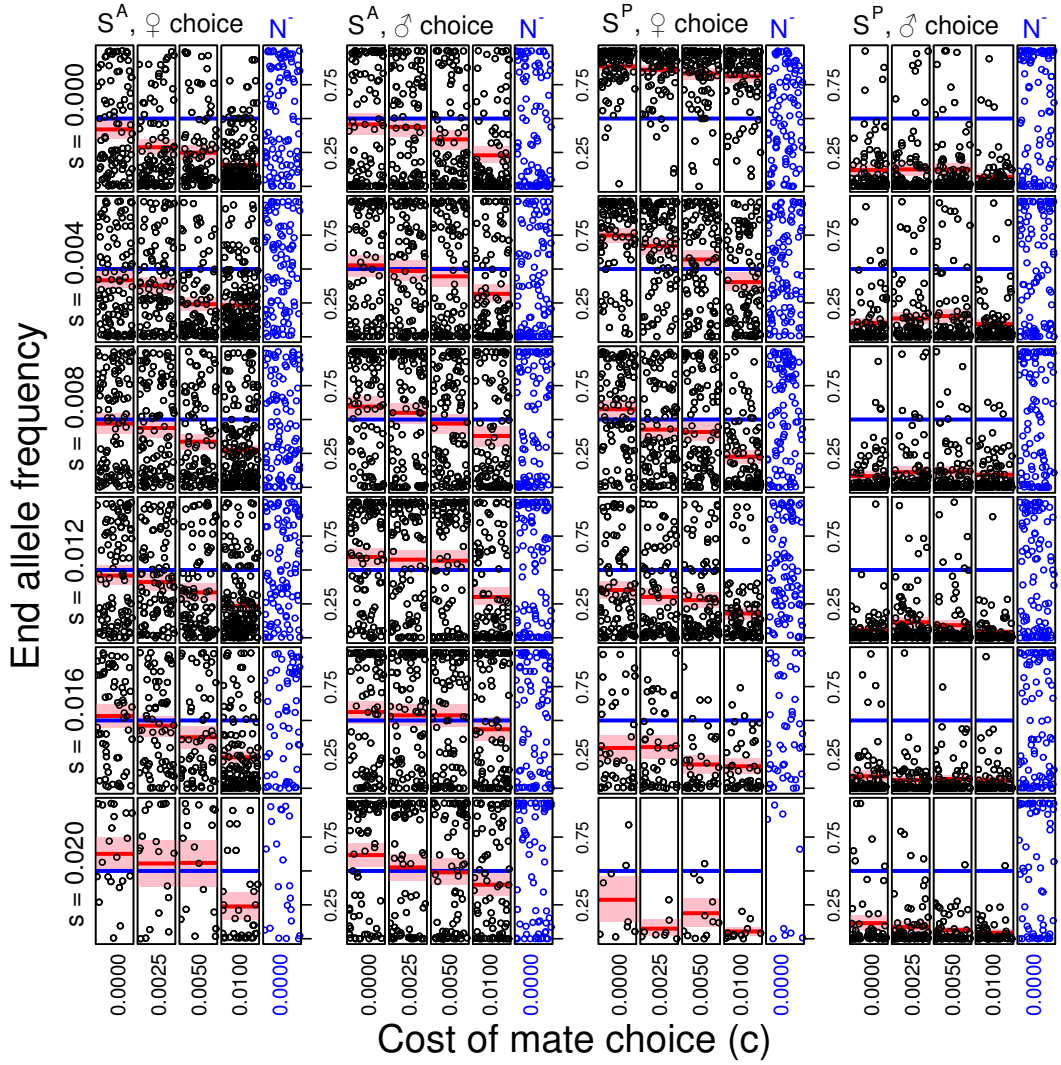

Figure S8: Distributions of end allele frequencies with identical parameter combinations as in primary simulations, but where only full and half siblings are recognised as kin, and therefore inbreeding with non-sibling kin cannot be avoided or preferred. For comparison, Figure 1 shows identical parameter combinations where kin discrimination is perfect. Overall, these extended results show that restricting kin recognition to full or half siblings can strongly restrict the evolution of inbreeding avoidance or preference. For example, given female choice, mean S^A end frequencies never exceed 0.5, and thus selection for inbreeding avoidance is never inferred. Inbreeding avoidance was inferred when males chose, but end S^A frequencies were not as consistently near fixation as when kin discrimination was perfect. In contrast, end S^P frequencies were consistently higher when kin discrimination was restricted rather than perfect and females chose, but this was due the assumption that immigrant allele frequencies were identical to those of the native population (see Discussion of the main text). When males chose, however, S^P end values were consistently lower when kin discrimination was restricted.

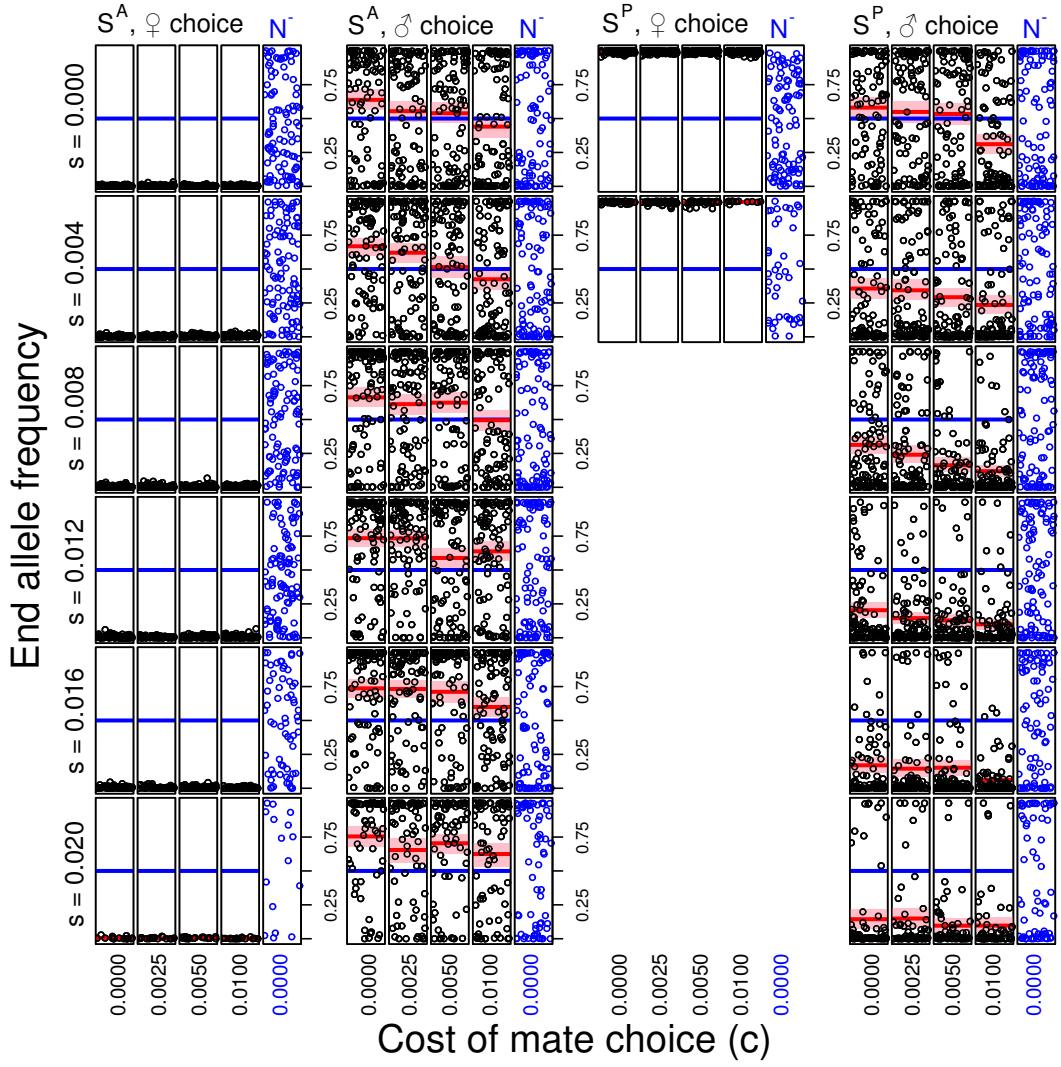

Figure S9: Distributions of end allele frequencies with identical parameter combinations as in primary simulations, but the perceived quality of the non-choosing sex is affected by S^A or S^P alleles in both sexes. Specifically, when females chose, related males carrying S^P increased their own perceived quality, and related males carrying S^A decreased their own perceived quality. For comparison, Figure 1 shows identical parameter combinations when the non-choosing sex does not affect its own quality. Overall, allowing the non-choosing sex's alleles to affect whether or not it was chosen as a mate greatly affected end allele frequencies when females, but not males chose. Because females are resource-limited, they are always assured to mate and produce n offspring, so inbreeding avoidance or preference had little effect on allele transmission when males were the choosing sex but females affected their own quality. In contrast, males that increased or decreased their perceived quality by causing females relatives to prefer (S^P) or avoid (S^A) them greatly increased (S^P carriers) or decreased (S^A carriers) their reproductive success. Strong selection for S^P increased inbreeding depression and therefore population extinction.

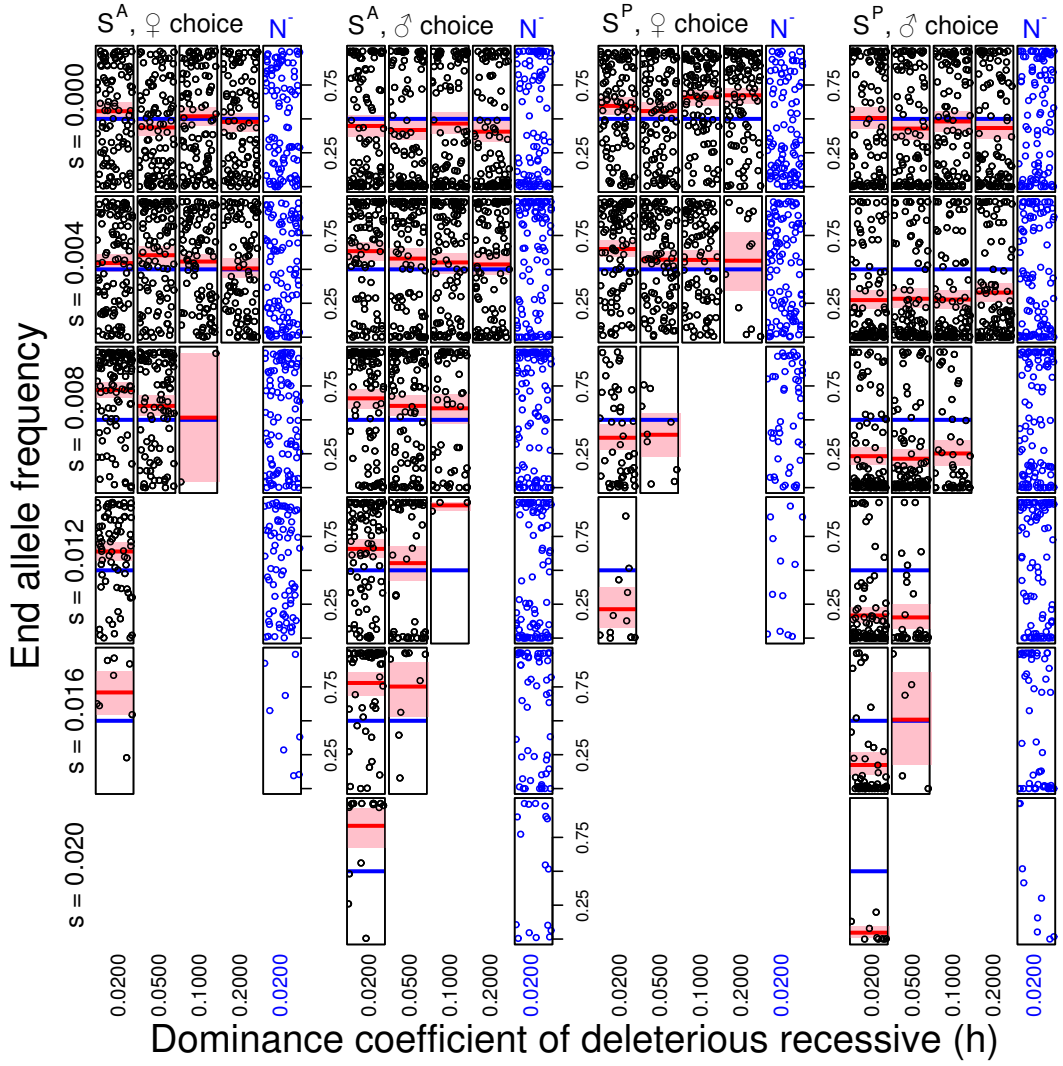

Figure S10: Effect of dominance coefficient (h) of deleterious recessive alleles on end allele frequencies. This figure is interpreted the same way as that of Figure 1, but here small inner columns show simulations with different h values. In all simulations, no direct costs of inbreeding strategy are modelled ($c = 0$), so comparison to the default $h = 0$ is possible in Figure 1 where $c = 0$. Overall, h had no qualitative effect on end allele frequencies; the possible trend for S^P where females chose and $s = 0$ is not significant when $h = 0$ is included ($P = 0.165$). High h increased the probability of population extinction; boxes are not shown where no simulations persisted to 3000 generations.

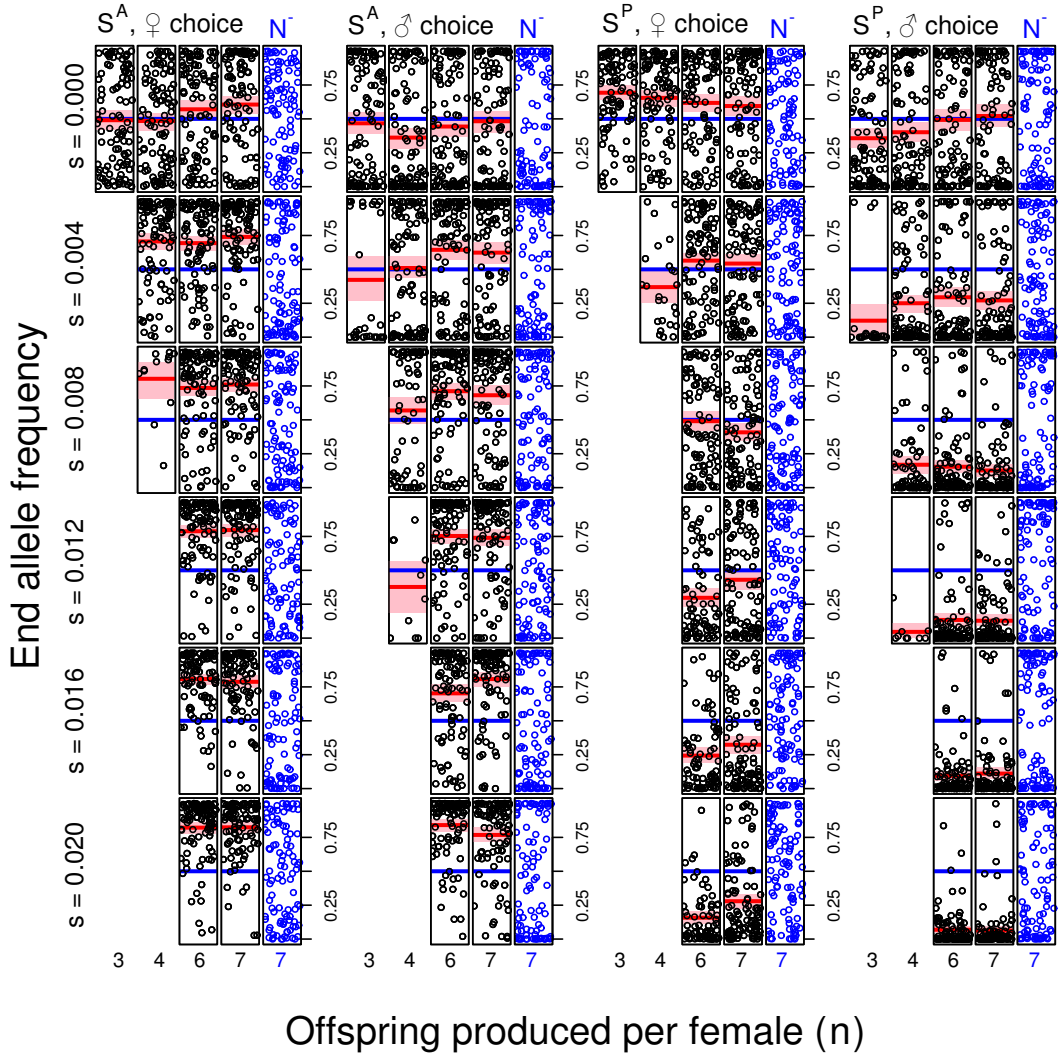

Figure S11: Effect of offspring produced per female (n) on end allele frequencies. This figure is interpreted the same way as Figure 1, but small inner columns show simulations with different n values. In all simulations, direct cost of inbreeding strategy was zero ($c = 0$), so comparison to the default $n = 5$ is possible in Figure 1 where $c = 0$. Overall, n had no qualitative effect on end allele frequencies, but low values of n led to population extinction because not enough offspring were produced for a positive population growth rate. This occurred where no boxes are shown indicating that no simulations persisted to 3000 generations. For larger values of $n > 4$, populations always persisted, as is evident from multiple points within boxes.

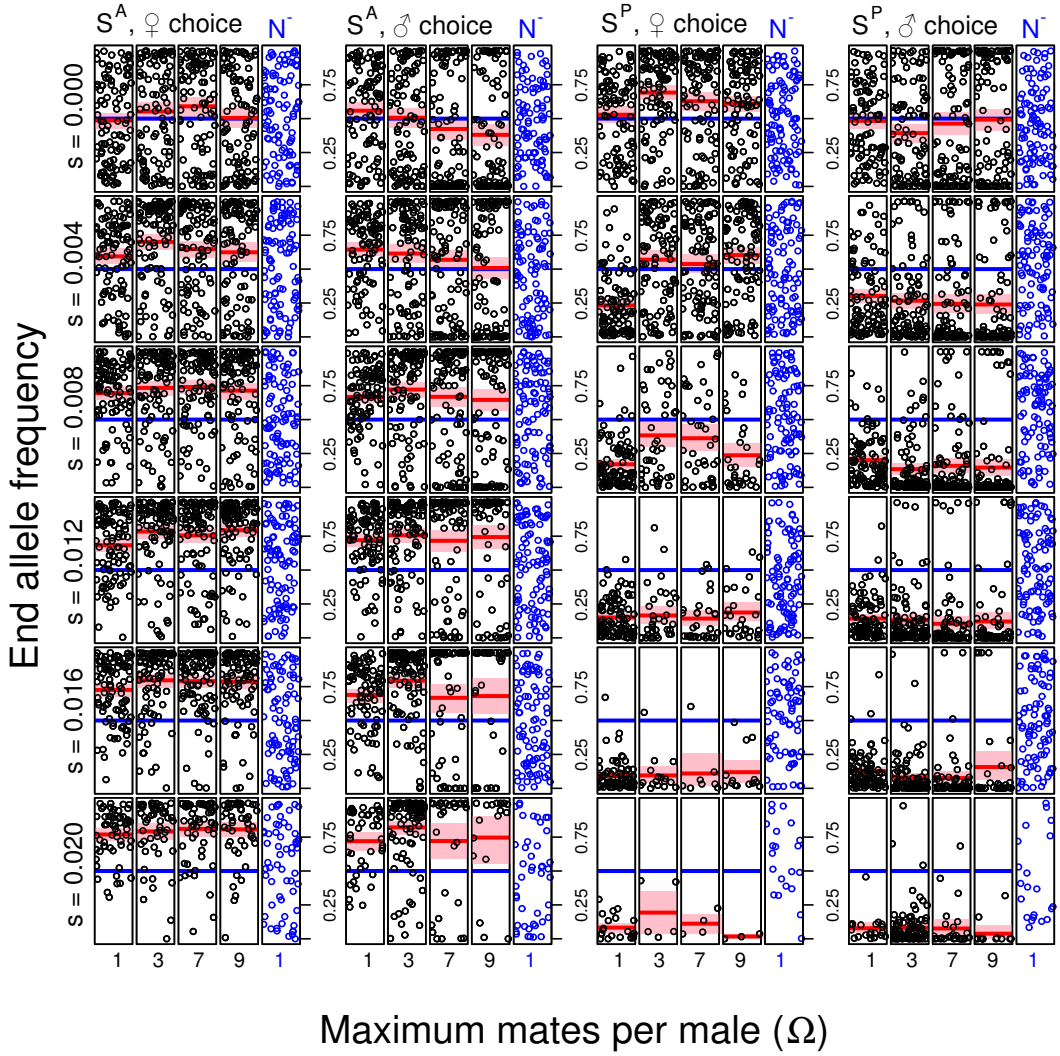

Figure S12: Effect of maximum mates per male (Ω) on end allele frequencies. This figure is interpreted the same way as Figure 1, but small inner columns show simulations with different Ω values. In all simulations, direct cost of inbreeding strategy was zero ($c = 0$), so comparison to the default $\Omega = 5$ is possible in Figure 1 where $c = 0$. Overall, Ω had no qualitative effect on end allele frequencies where $\Omega > 1$. The special case where $\Omega = 1$ is notable because it represents a case in which both sexes could mate only once and reproductive success is therefore expected to be identical. Here, end allele frequencies did not differ between females and males, and this is especially apparent for S^P simulations when females chose. When $\Omega > 1$, selection for S^P was sometimes expected because female inbreeding preference increased the reproductive success of male relatives. Yet selection for S^P was never expected when $\Omega = 1$ and females chose for the same reason that selection for S^P was never expected at all when males chose; female inbreeding preference cannot increase the reproductive success of male relatives if $\Omega = 1$.

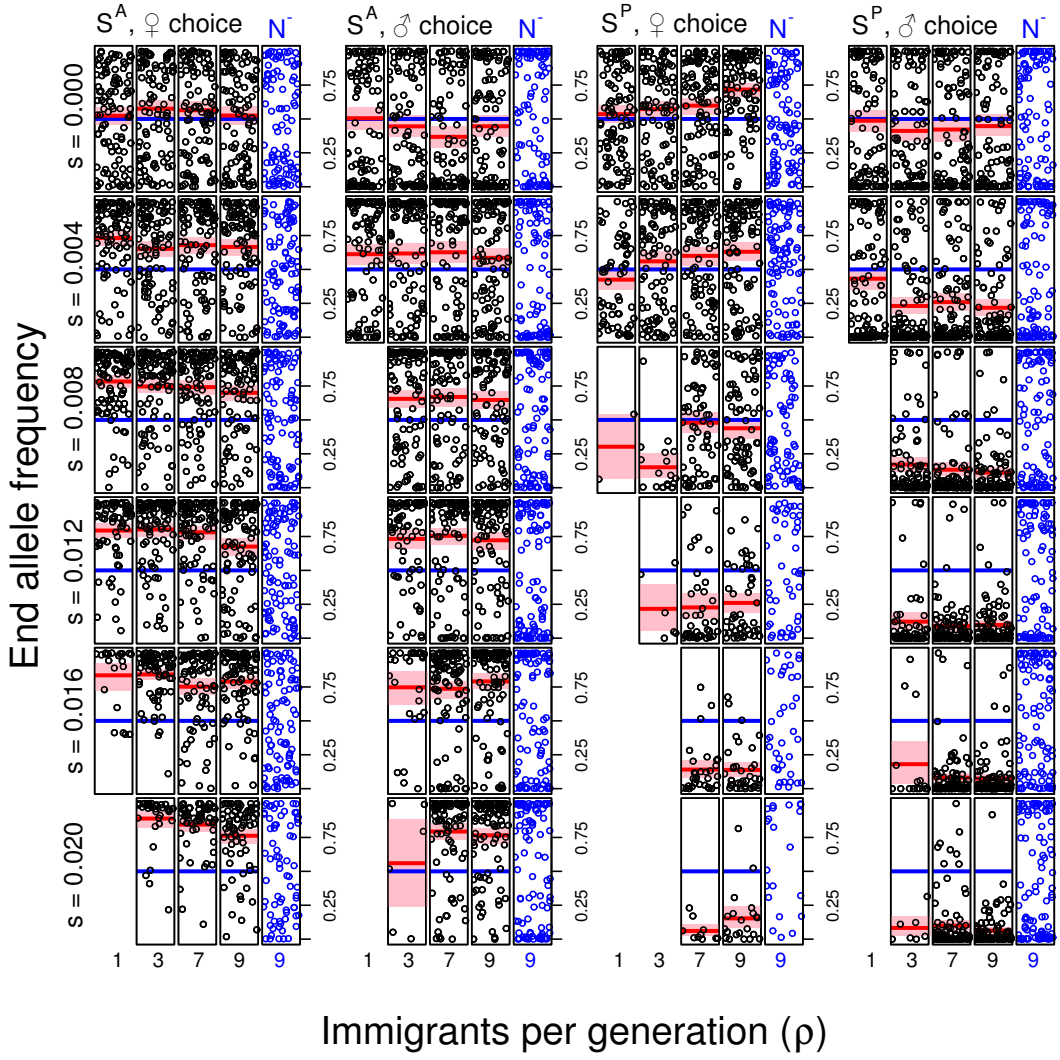

Figure S13: Effect of the number of immigrants per generation (ρ) on end allele frequencies. This figure is interpreted the same way as Figure 1, but small inner columns show simulations with different ρ values. In all simulations, direct cost of inbreeding strategy was zero ($c = 0$), so comparison to the default $\rho = 5$ is possible in Figure 1 where $c = 0$. Overall, ρ had no qualitative effect on end allele frequencies, but low values of ρ led to population extinction at high s values due to higher population-wide inbreeding coefficients and hence greater expression of inbreeding depression when immigration rate was low.

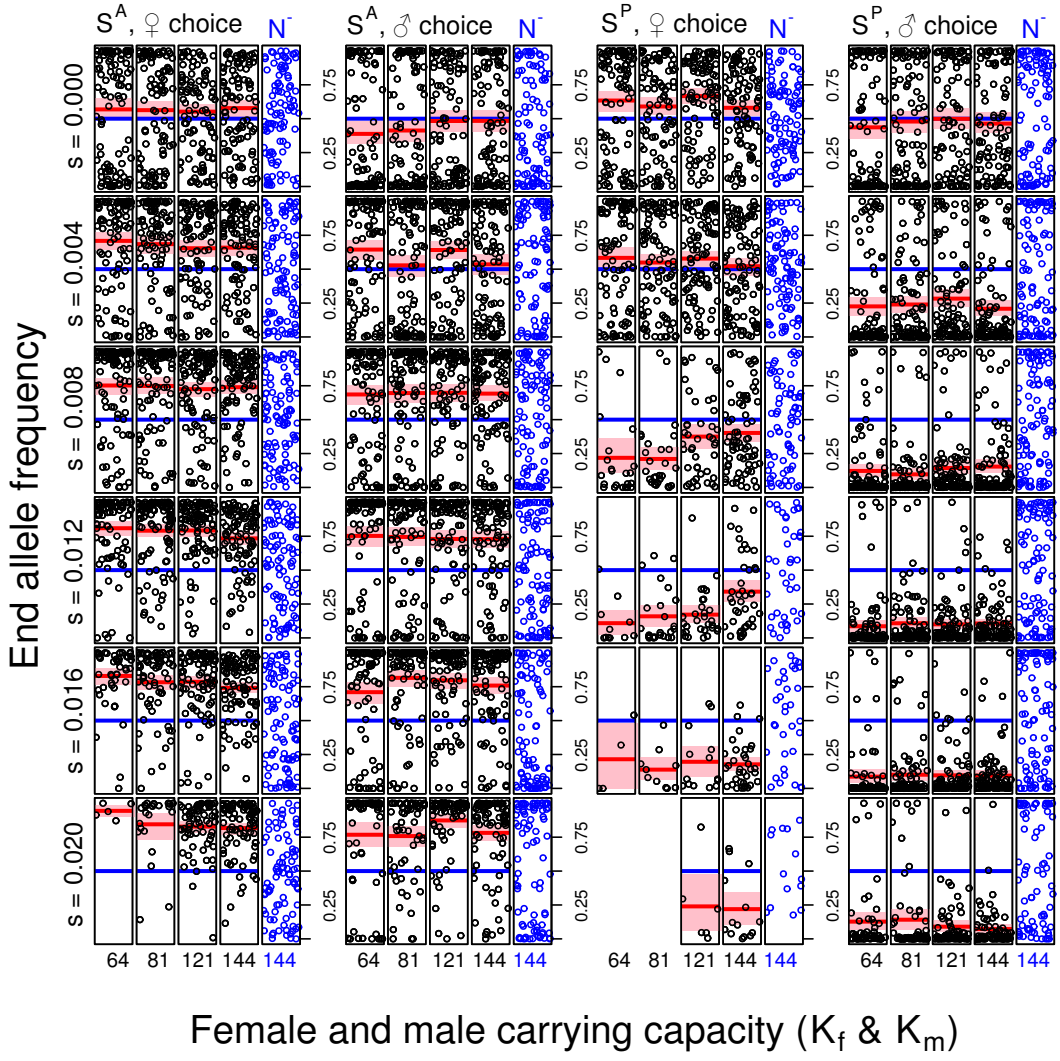

Figure S14: Effect of female and male carrying capacities (K_f & K_m), which are always set to equal values, on end allele frequencies. This figure is interpreted the same way as Figure 1, but small inner columns show simulations with different $K_f = K_m$ values. In all simulations, direct cost of inbreeding strategy was zero ($c = 0$), so comparison to the default $K_f = K_m$ is possible in Figure 1 where $c = 0$. Overall, $K_f = K_m$ had no qualitative effect on end allele frequencies across this range of 64-144, but as $K_f = K_m$ increased to higher values, end S^A allele frequencies decreased to mean values of 0.5, as expected if alleles were neutral. The reason for this decrease is explained in detail in terms of effective population size N_e in the main text (see Figure 5); at very high population sizes, fewer close relatives were encountered relative to distant or non-relatives. Low $K_f = K_m$ also resulted in more frequent population extinction (fewer points within boxes, or the empty boxes where S^P and females chose).

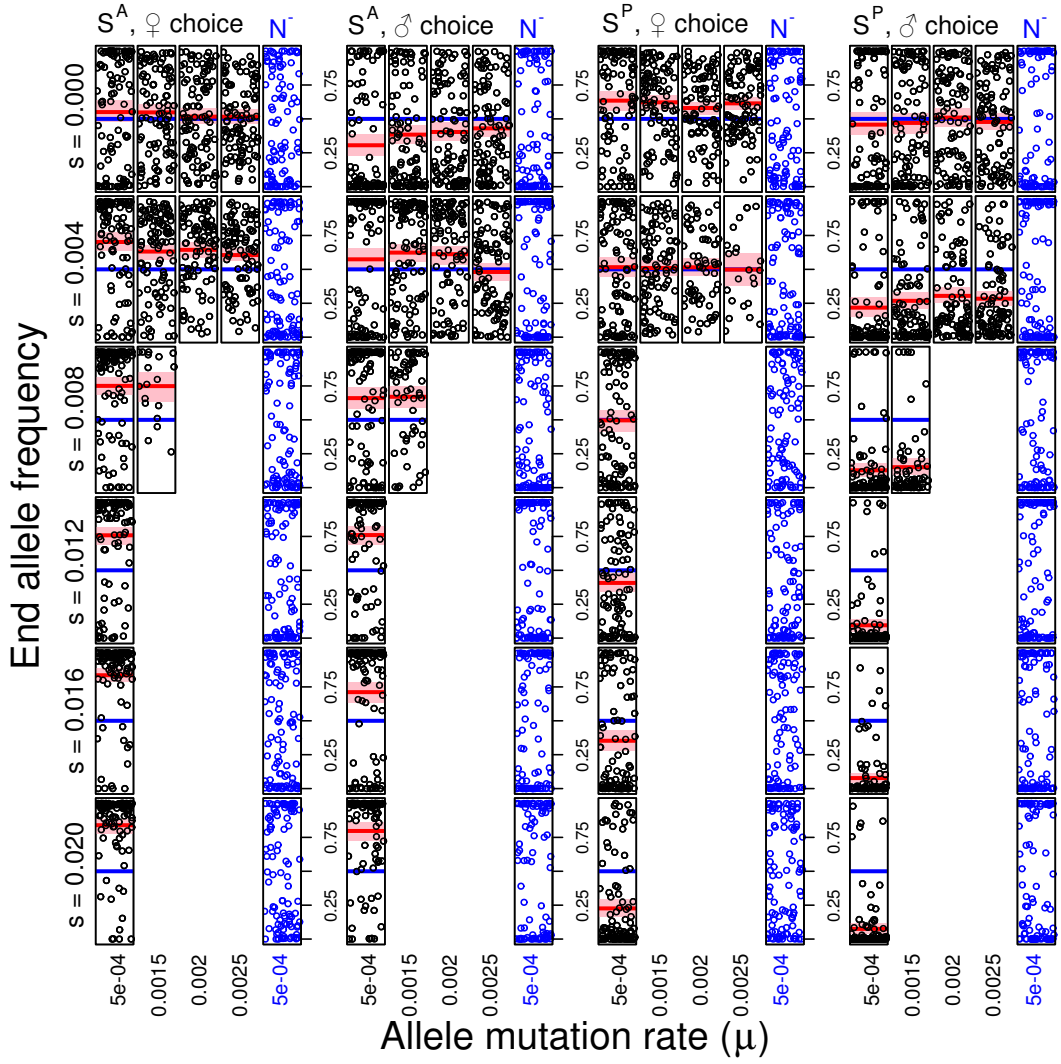

Figure S15: Effect of allele mutation rate (μ) on end allele frequencies. This figure is interpreted the same way as Figure 1, but small inner columns show simulations with different μ values. In all simulations, direct cost of inbreeding strategy was zero ($c = 0$), so comparison to the default $\mu = 0.001$ is possible in Figure 1 where $c = 0$. Overall, μ did not qualitatively effect end allele frequencies, but high μ led to frequent population extinction as wild-type alleles at the load loci (L^+) mutated frequently to deleterious recessive alleles (L^-), increasing inbreeding depression and therefore extinction (verified by regressing L^- end frequencies against μ, $P < 0.001$).

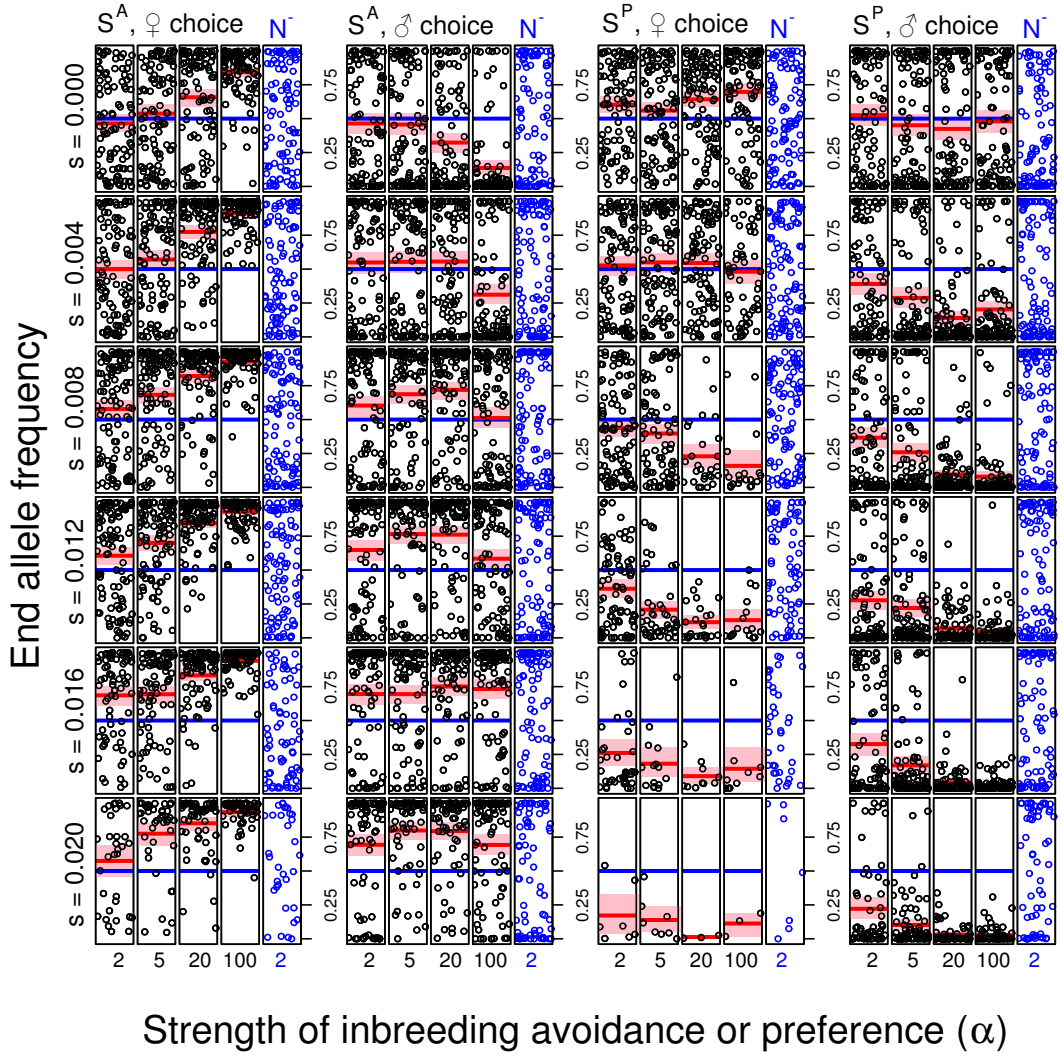

Figure S16: Effect of the strength of allele effects (α) on end allele frequencies. This figure is interpreted the same way as Figure 1, but small inner columns show simulations with different α values. In all simulations, direct cost of inbreeding strategy was zero ($c = 0$), so comparison to the default $\alpha = 10$ is possible in Figure 1 where $c = 0$. Overall, the value of α tended to increase the strength of selection, so while the strength of α did not generally change whether or not selection increased, decreased, or had no effect on alleles, it did affect mean end allele frequencies. This is unsurprising; when an allele that increases or decreases inbreeding is under directional selection, increasing the strength of the allele's effect also increases the strength of selection relative to drift. Hence where $\alpha = 100$, end mutant alleles are more often driven to extinction or fixation. Interestingly, given S^A where females chose (left-most large column), end S^A increases with α even in the absence of selection ($s = 0$). On inspection, this increase was found to be caused by a runaway process of inbreeding avoidance (see page S20).

Runaway evolution of inbreeding avoidance

In the absence of inbreeding depression in offspring survival ($s = 0$) and when females chose mates, S^A often reached a higher end frequency after 3000 generations than expected for a completely neutral allele, especially when the strength of the effect of alleles underlying inbreeding avoidance (α) was high (Figure S16). This led to fixation of S^A in a relatively high proportion of populations. This requires some explanation because in the absence of inbreeding depression, inbred and outbred offspring are expected to be equally fit, so there is no obvious reason to expect inbreeding avoidance to be beneficial.

By examining the dynamics of individual simulations, we found evidence of a positive correlation between the degree to which females avoided inbreeding and their sons' subsequent fecundity (reproductive success), leading to a positive feedback (runaway) that increased the frequency of S^A. Figure S17 illustrates this process when $\alpha = 25$ and S^A increases from zero to near fixation. Females carrying S^A are less closely related to their mates than females carrying S^+. In Figure S17B, the correlation between maternal genotype and the degree to which her son's mean kinship with individuals within the population deviates from the overall mean among-individual kinship is shown over time. Specifically, females that avoided inbreeding were more likely to mate with males that were more distantly related to the average individual within the population. The negative correlation between a mother genotype and son deviation in mean kinship (black line Figure S17B) indicates that mothers with S^A produced sons that were less closely related to the rest of the population than sons produced by mothers with S^+ alleles. Simultaneously, the red line in Figure S17B indicates that the deviation of a male's mean kinship with the population from the overall population mean kinship was negatively correlated with male reproductive success. In other words, males that were relatively less closely related to the rest of the population had more offspring because they were more likely to be selected as mates.

This process by which inbreeding avoidance evolves due to a positive correlation between mother genotype and son reproductive success (in the absence of inbreeding depression) is conceptually interesting (and, to our knowledge, conceptually novel) because it suggests that inbreeding avoidance, like other reproductive strategies, could potentially evolve through self-perpetuating runaway. Nevertheless, the effect seems likely to be too weak to drive evolution in nature, especially relative to the fitness effects of inbreeding depression and direct costs associated with active inbreeding strategies. Further, in addition to assuming no inbreeding depression or inbreeding avoidance costs, simulations such as those in Figure S17 assume that only inbreeding avoidance can evolve from inbreeding tolerance. But given low or negligible inbreeding depression and direct costs, inbreeding preference might be more likely to evolve when females have control over mating.

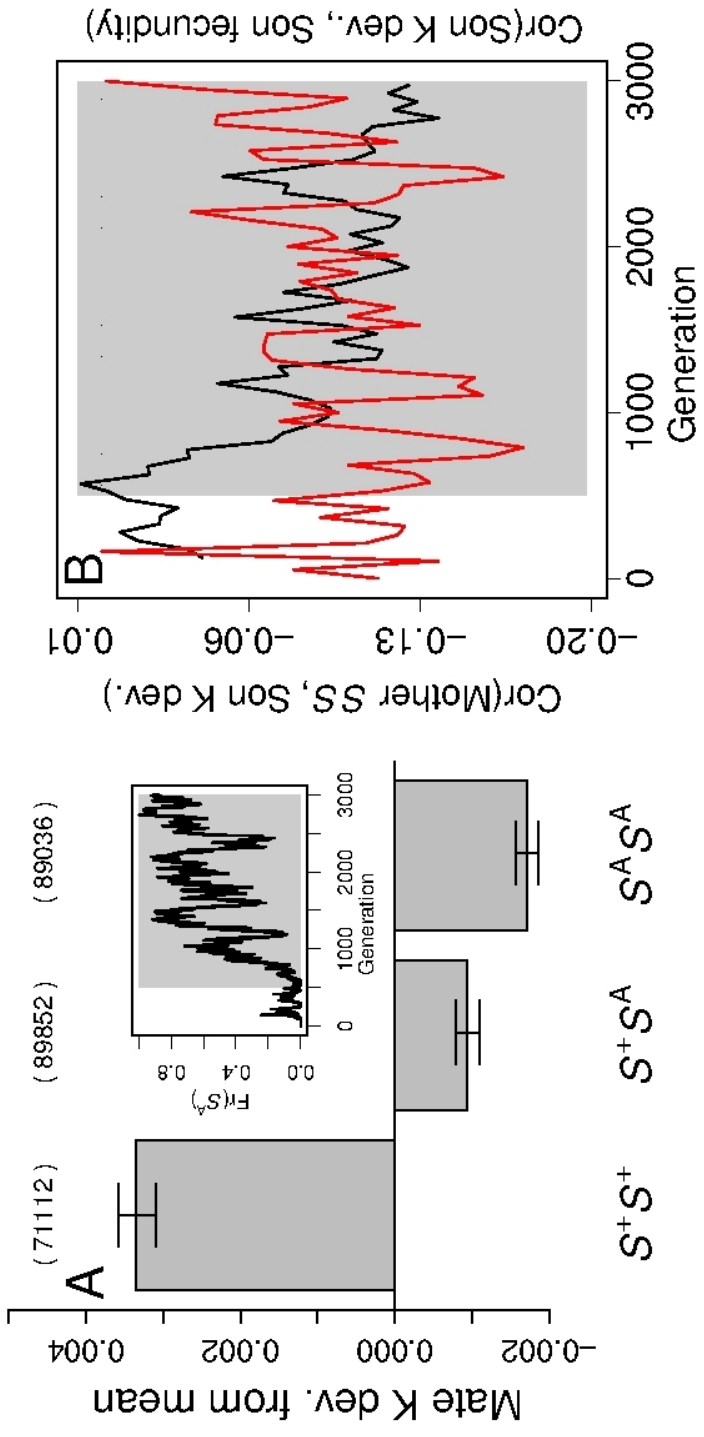

Figure S17: Dynamics of a mutant allele underlying inbreeding avoidance (S^A) given no inbreeding depression in offspring survival ($s = 0$). Plot (A) shows the deviation in kinship between a focal female and her selected mate from that of the mean kinship between mates in the same generation for 100000 females of each genotype sampled from the last 2500 generations of the simulation (shaded region of line plot; error bars show 95% bootstrapped confidence intervals). The plot in (A) shows the frequency of S^A ($Fr\left(S^A\right)$) over 3000 generations. The left axis and black line of (B) shows the correlation between mothers' genotypes ($S^+S^+ = 0$, $S^+S^A = 0.5$, $S^AS^A = 1$) and the degree to which their sons' kinships differ from the mean kinship within the population in a generation. The right axis and red line of (B) shows the correlation between sons' deviation from the mean kinship of the population and the number of offspring sons produce. In both axes of (B), mean values are binned for every 50 generations to facilitate interpretation.

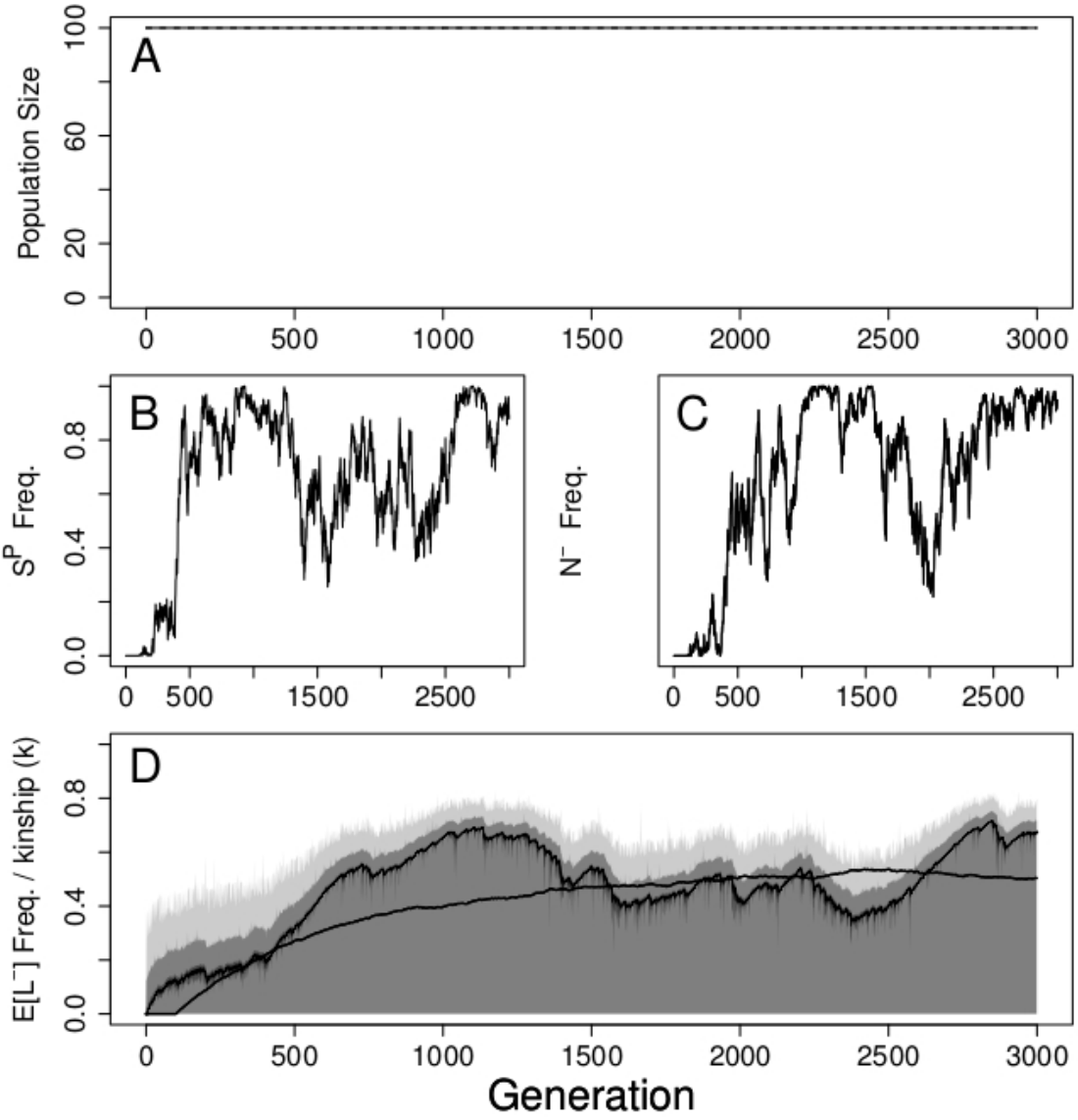

Figure S18: An example of the dynamics of (A) population size, (B) inbreeding preference allele (S^P) and (C) neutral allele (N^-) frequencies, and (D) the distribution of pairwise kinship values and mean deleterious recessive allele frequencies over 3000 generations. In A, population size is always at carrying capacity ($K_f = K_m = 100$) for both females and males. In D, the thin black line illustrates the mean frequency of L^- alleles across 1000 loci. Shading indicates the distribution of kinship between all pairwise combinations of individuals, where increasingly lighter shades encompass a higher proportion of kinships. Black, dark grey, mid grey, and light grey encompass 75%, 90%, 99%, and 100% of all kinships, respectively. Parameters are set at default values given zero selection against deleterious recessives ($s = 0$) and zero direct costs ($c = 0$), and females are the choosing sex; higher s and c values, or males being the choosing sex, resulted in stable kinship distributions.